

Optimal Thickness of a Cylindrical Shell – Shape Optimization with Time-dependent Force

Peter Nestler

Communicated by Zenon Mróz

September 25, 2012

Abstract

We discuss shape optimization problems for cylindrical tubes that are loaded by time-dependent applied force. This is a problem of shape optimization that leads to optimal control in linear elasticity theory. We determine the optimal thickness of a cylindrical tube minimizing the deformation of the tube under the influence of the external force. The main difficulty is that the state equation is a hyperbolic partial differential equation of 4th order. First order necessary conditions for the optimal solution are derived. Based on them, a numerical method is set up and numerical examples are presented.

Keywords: Calculus of variations and optimal control · Problems involving ordinary differential equations · Optimization of shapes other than minimal surfaces

1 Introduction

The present paper considers the effect of an external rotationally and symmetric force on a cylindrical shell. This force depends on time and space. The reader might imagine an explosion in a certain region of a pipeline. It is, by the way, one application that stands behind the problem. As a result of this force the cylinder tube is deformed. Our objective is to determine the thickness of the tube, that minimizes the deformation. The underlying physical process is described by a hyperbolic partial differential equation with boundary and initial conditions, which results from the law of conservation of momentum.

As an additional condition, we require that the volume of the tube remains constant. To obtain practical solutions we also assume the thickness to vary only within specified limits. To determine an optimal thickness numerically and we derive first order necessary conditions for the optimal solution. The

particular way of numerical treatment is one of our main issues. Moreover, the first-order conditions for optimality are tested numerically to evaluate the precision of the computed optimal shape. The main novelty of this work is that, we treat the transient case, which is formulated in the next section.

In this way, we extended our investigation in [1], where we discussed a simpler problem of this topic, namely the stationary case. For a short survey on the history of this particular problem, we refer the reader to [1]. We only mention the papers R. T. Haftka et al [2] and Z. Mróz [3], that are related to our problems.

The main novelty in comparison with [1] is that the state equation is now a hyperbolic partial differential equation of 4th order and the associated optimal control problems are more complex. To prove necessary optimality conditions for optimality is now essentially more difficult. Also the numerical simulations are more expensive and time consuming.

The main theoretical tool for establishing our optimality conditions is adjoint calculus. We should mention that the use of adjoint methods in the numerical analysis of optimal shape design problems already has a long history and numerous publications were devoted to this topic. We only refer to [4],[5],[6] with a stronger focus on the analysis of the problems and to R. T. Haftka et al [2], Z. Mróz [3], or G. Rozvany [7], who are shed more light on the mechanics of the problems but also derive first order necessary optimality conditions and discuss their numerical use.

Notice that, due to the presence of a hyperbolic state equation, the analysis of first order conditions is more delicate for our class of problems. The associated analysis is one of our major issues, even through we do not present all details to shorten the presentation. Details can be found in [1].

2 Modeling of the Problem

We first state some very preliminary notions of elasticity theory, detailed information can be found in standard books on this topic [8,9,10]. We also refer to the discussion in [1] that is related to this paper.

Let $\bar{\Omega}_{3D} \subset \mathbb{R}^3$ be the reference configuration for a body in the stress free state. The state is expressed by a map $\phi : \bar{\Omega}_{3D} \rightarrow \mathbb{R}^3$. This map includes the identity mapping and small displacements \mathbf{y} . The deviation from the identity mapping is expressed by the strain. The strain-tensor ε has the components

$$\varepsilon_{ij} = \frac{1}{2} \left(\frac{\partial y_i}{\partial x_j} + \frac{\partial y_j}{\partial x_i} \right) \quad i, j = 1, 2, 3.$$

The displacements depend on material parameters by Hooke's law

$$\sigma(\mathbf{y}) = 2\mu \varepsilon(\mathbf{y}) + \lambda(\text{trace}(\varepsilon(\mathbf{y}))) \cdot I,$$

with the Lamé-constants λ, μ (material parameters), the identical tensor I , and the stress tensor σ .

We derive our system equation from the principle of minimizing the energy functional

$$\Pi(\mathbf{y}) := \int_{\Omega_{3D}} \left[\frac{1}{2} \sigma(\mathbf{y}) : \varepsilon(\mathbf{y}) - \mathbf{f} \cdot \mathbf{y} \right] d\mathbf{x} - \int_{\partial\Omega_{3D}} \mathbf{g} \cdot \mathbf{y} dS$$

for all admissible \mathbf{y} . The term $\sigma : \varepsilon$ denotes the second order tensor product of σ and ε . The function \mathbf{f} represents the force exerted on the body and \mathbf{g} formulates possible boundary conditions derived from the specific problem. For modeling the cylindrical shell we use the hypotheses of Mindlin and Reissner [8,9]. This allows to reduce our 3-dimensional problem to a 1-dimensional. The deformation of the body under a force \mathbf{f} is modeled by the balance of power

$$-\operatorname{div} \sigma(\mathbf{y}) = \mathbf{f}.$$

In the transient case, the small displacements $\mathbf{y} : \Omega_{3D} \times [0, T] \rightarrow \mathbb{R}$ depend also on the time. We will use the law of conservation of momentum

$$\rho \partial_t^2 \mathbf{y} = \operatorname{div} \sigma(\mathbf{y}) + \mathbf{f}, \quad (1)$$

with the density ρ as starting point for modeling. Invoking also the hypotheses of Mindlin and Reissner, we transform the 3-dimensional reference domain problem to 1-dimensional domain problem.

Next, we introduce the cylindrical shell to be optimized. A cylindrical shell is most conveniently described in cylindrical coordinates. The surface of the cylinder $\Omega_{2D}^C := [0, 1] \times [0, 2\pi]$ with radius R is given by

$$\mathbf{z}(x, \varphi) = \begin{bmatrix} x \\ R \cos \varphi \\ R \sin \varphi \end{bmatrix}, \quad x \in \bar{\Omega} := [0, 1], \varphi \in [0, 2\pi].$$

The cylindrical shell \mathcal{S} with center plane $\mathbf{z}(x, \varphi)$ and thickness u is given by

$$\mathcal{S} = \left\{ \mathbf{z}(x, \varphi) + h \begin{bmatrix} 0 \\ \cos \varphi \\ \sin \varphi \end{bmatrix} \mid h \in \left[-\frac{u}{2}, \frac{u}{2} \right], (x, \varphi) \in \Omega_{2D}^C \right\},$$

in the natural coordinate system \mathbf{e}_i , $i \in \{1, 2, 3\}$, specified by the cylindrical shell,

$$\mathbf{e}_1 = \frac{\partial \mathcal{S}}{\partial x} \quad \mathbf{e}_2 = \frac{\partial \mathcal{S}}{\partial \varphi} \quad \mathbf{e}_3 = \frac{\partial \mathcal{S}}{\partial h}.$$

We mention that $\Omega_{3D} = \mathcal{S}$, to close the gap to the setting above.

The hypotheses of Mindlin and Reissner lead to the displacement law in the natural basis \mathbf{e}_i $i \in \{1, 2, 3\}$:

$$\mathbf{y} = y_1(x, \varphi, t) \mathbf{e}_1 + y_2(x, \varphi, t) \mathbf{e}_2 + y_3(x, \varphi, t) \mathbf{e}_3 - h[\theta_1(x, \varphi, t) \mathbf{e}_1 + \theta_2(x, \varphi, t) \mathbf{e}_2]$$

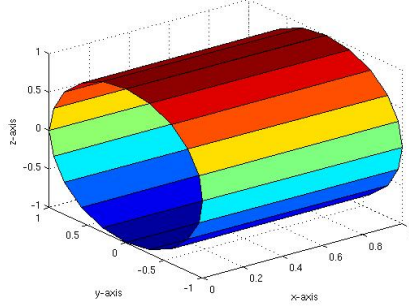


Figure 1: cylindrical shell

where $y_i : \mathcal{S} \times (0, T] \rightarrow \mathbb{R}$ are the displacements with respect to all basis-directions and we have torsions $\theta_i : \mathcal{S} \times (0, T] \rightarrow \mathbb{R}$. We assume a rotationally symmetric force. Let the tube be fixed at its ends and let the Kirchhoff-Love hypothesis for a thin shell be fulfilled. This hypothesis implies

$$y_1 = y_2 = \theta_2 = 0 \text{ and } \partial_x y_1 = \theta_1$$

for all t in $[0, T]$. We use soft clamped boundary conditions ($y_i = 0, \nabla \theta_i = 0$ for all t on the considered boundary) which are often considered in practice. The displacement law is substituted into the momentum conservation law (1). With $w_o := y_3$ and $f_z := \mathbf{f} \cdot \mathbf{e}_3$ we end up with the equations for the transient problem in weak formulation. We define the solution space

$$\mathbb{W}_o(0, T) := \{w_o \in \mathbb{L}^2(0, T; \mathbb{V}), \partial_t w_o \in \mathbb{L}^2(0, T; \mathbb{H}_0^1(\Omega)), \partial_t^2 w_o \in \mathbb{L}^2(0, T; \mathbb{V}^*)\}$$

with $\mathbb{V} := \mathbb{H}^2(\Omega) \cap \mathbb{H}_0^1(\Omega)$ and $\partial_t^2 w_o$ as distributional derivative. Here and in what follows, $\partial_t w_o$ stands for $\partial w_o / \partial t$. The space $\mathbb{H}^k(\Omega)$ denotes the standard Sobolev space of order k and $\mathbb{L}^2(0, T; \mathbb{V})$ is the space of abstract Lebesgue measurable functions with images in \mathbb{V} . We recall that $\Omega = (0, 1)$.

Original problem: Find a solution $w_o \in \mathbb{W}_o(0, T)$ that fulfills the equations

$$\int_{\Omega} \left\{ \rho \left(Ru \partial_t^2 w_o \tilde{w} + \frac{Ru^3}{12} \partial_t^2 \partial_x w_o d_x \tilde{w} \right) + (2\mu + \lambda) \left[\frac{Ru^3}{12} \partial_x^2 w_o d_x^2 \tilde{w} + \left(\frac{u^3}{12R^3} + \frac{u}{R} \right) (w_o \tilde{w}) \right] \right\} dx = R \int_{\Omega} f_z \tilde{w} dx \quad (2)$$

for each $\tilde{w} \in \mathbb{V}$ and for almost all $t \in (0, T)$ with initial data $w_o = 0$ in \mathbb{V} and $\partial_t w_o(0) = 0$ in $\mathbb{H}_0^1(\Omega)$. We use $d_x^2 \tilde{w}$ instead $d^2 \tilde{w} / dx^2$. For a proof of the existence of a solution of the derived equations, we need the assumptions below and define a family of continuous bilinear forms on \mathbb{V} ,

$$a(t; w_o, \tilde{w}) := (2\mu + \lambda) \left[\frac{Ru^3}{12} \partial_x^2 w_o d_x^2 \tilde{w} + \left(\frac{u^3}{12R^3} + \frac{u}{R} \right) (w_o \tilde{w}) \right] dx.$$

Assumptions 2.1. 1) The function $t \rightarrow a(t; w_o, \tilde{w})$ is for all w_o, \tilde{w} in \mathbb{V} once continuously differentiable in $[0, T]$, with $T < \infty$.

2) There holds the symmetry $a(t; w_o, \tilde{w}) = a(t; \tilde{w}, w_o)$ and, for some $\lambda \in \mathbb{R}$,

$$a(t; w_o, w_o) + \lambda |w_o| \geq \alpha \|w_o\|_{\mathbb{V}}^2, \quad \alpha > 0 \quad \forall w_o \in \mathbb{V}.$$

We consider the problem (2) by a variational formulation in the Gelfand triple $(\mathbb{V}, \mathbb{L}^2(\Omega), \mathbb{V}^*)$:

$$\left(\rho R u \partial_t^2 w_o, \tilde{w} \right)_{\mathbb{L}^2} + \left(\rho \frac{R u^3}{12} \partial_t^2 \partial_x w_o, d_x \tilde{w} \right)_{\mathbb{L}^2} + a(t; w_o, \tilde{w}) = (R f_z, \tilde{w})_{\mathbb{L}^2}.$$

Theorem 2.1. *Assume that assumptions (2.1) hold. Let $f_z \in \mathbb{L}^2(0, T; \mathbb{V})$, $w_o(0) \in \mathbb{V}$ and $\partial_t w_o(0) \in \mathbb{H}_0^1(\Omega)$ be given. Then exists a unique solution w_o in $\mathbb{W}_o(0, T)$ of (2). The mapping $\{f_z, w_o(0), \partial_t w_o(0)\} \rightarrow \{w_o, \partial_t w_o\}$ is continuous and linear from $\mathbb{L}^2(0, T; \mathbb{V}) \times \mathbb{V} \times \mathbb{H}_0^1(\Omega)$ to $\mathbb{L}^2(0, T; \mathbb{V}) \times \mathbb{L}^2(0, T; \mathbb{H}_0^1(\Omega))$.*

We omit the proof of this theorem that is long and technical. For the proof and additional information, we refer to [11], where also general results of [12,13] are used.

The term with the mixed derivative $\partial_t^2 \partial_x w_o d_x \tilde{w}$ is neglected in most cases that are interesting for mechanical applications. Then it follows a simplified equation for the transient case. First we define the associated solution space

$$\mathbb{W}_s(0, T) := \{w_s \in \mathbb{L}^2(0, T; \mathbb{V}), \partial_t w_s \in \mathbb{L}^2(0, T; \mathbb{L}^2(\Omega)), \partial_t^2 w_s \in \mathbb{L}^2(0, T; \mathbb{V}^*)\}$$

In what follows, the subscripts "o" and "s" stand for original and simplified problem.

Simplified problem: Find a solution $w_s \in \mathbb{W}_s(0, T)$ that fulfills the equations

$$\int_{\Omega} \left\{ \rho R u \partial_t^2 w_s \tilde{w} + (2\mu + \lambda) \left[\frac{R u^3}{12} \partial_x^2 w_s d_x^2 \tilde{w} + \left(\frac{u^3}{12R^3} + \frac{u}{R} \right) (w_s \tilde{w}) \right] \right\} dx = R \int_{\Omega} f_z \tilde{w} dx \quad (3)$$

for each $\tilde{w} \in \mathbb{V}$ and for almost all $t \in (0, T)$ with initial data $w_o = 0$ in \mathbb{V} and $\partial_t w_o(0) = 0$ in $\mathbb{L}^2(\Omega)$. Numerical tests have shown for constant coefficients that the influence of the mixed derivative of the solution w_o can be neglected. Also for this problem, we have an existence theorem.

Theorem 2.2. *Assume that assumptions (2.1) hold. Let $f_z \in \mathbb{L}^2(0, T; \mathbb{V})$, $w_s(0) \in \mathbb{V}$ and $\partial_t w_s(0) \in \mathbb{L}^2(\Omega)$ be given. Then exists a unique solution w_s in $\mathbb{W}_s(0, T)$ of (3). The mapping is continuous and linear from $\mathbb{L}^2(0, T; \mathbb{V}) \times \mathbb{V} \times \mathbb{L}^2(\Omega)$ to $\mathbb{L}^2(0, T; \mathbb{V}) \times \mathbb{L}^2(0, T; \mathbb{L}^2(\Omega))$.*

The proof of this theorem can be found in [11] as well. The variational formulations have the advantage weak solution $w_{o/s} \in \mathbb{W}_{o/s}(0, T)$ can be considered and the functions f_z need only to be square-integrable, i.e. $f_z \in \mathbb{L}^2(0, T; \mathbb{L}^2(\Omega))$. This generalization fits to practical problems. For the derivation of first order necessary conditions we additionally require the solutions w_o or w_s to have higher regularity. We can achieve this by demanding that the initial data $w_{o/s}(0), \partial_t w_{o/s}(0)$ and the right-hand side f_z have higher smoothness.

However, given initial data and the right-hand side at the initial time must be compatible. Thus the solutions belong to the following spaces:

$$\begin{aligned} w_{o/s} \in \mathbb{H}^1(0, T; \mathbb{V}) &:= \{w_{o/s} \in \mathbb{L}^2(0, T; \mathbb{V}), \partial_t w_{o/s} \in \mathbb{L}^2(0, T; \mathbb{V})\} \text{ or} \\ w_{o/s} \in \mathbb{H}^2(0, T; \mathbb{V}) &:= \{w_{o/s} \in \mathbb{H}^1(0, T; \mathbb{V}), \partial_t^2 w_{o/s} \in \mathbb{L}^2(0, T; \mathbb{V})\}. \end{aligned}$$

For more information on higher regularity for hyperbolic partial differential equation can be found in [11,12,13].

To cover the non-linearities with respect to the control u , we define Nemytskij operators $\Theta, \Upsilon, \Phi, \Psi : \mathbb{L}^\infty(\Omega) \rightarrow \mathbb{L}^\infty(\Omega)$:

$$\begin{aligned} \Theta(u) &:= \rho R u, & \Upsilon(u) &:= \frac{\rho R u^3}{12}, \\ \Phi(u) &:= (2\mu + \lambda) \frac{R u^3}{12}, & \Psi(u) &:= (2\mu + \lambda) \left(\frac{u^3}{12R^3} + \frac{u}{R} \right). \end{aligned}$$

These operators are continuously Frechét differentiable. Their derivatives can be expressed for a direction $h \in \mathbb{L}^\infty(\Omega)$ by

$$\begin{aligned} \Theta'(u)h &= \rho R h & \Upsilon'(u)h &= \frac{\rho R u^2}{4} h \\ \Phi'(u)h &= (2\mu + \lambda_{ESZ}) \frac{R u^2}{4} h & \Psi'(u)h &= (2\mu + \lambda_{ESZ}) \left(\frac{u^2}{4R^3} + \frac{1}{R} \right) h. \end{aligned}$$

3 Optimal Control Problems

The goal of optimization is to determine a thickness \bar{u} , that minimizes the deformation of the cylindrical tube. Additionally, we require the cylindrical shell to have a constant volume. For the formulation of the problem and its solvability, we assume the existence of an optimal control \bar{u} . To prove this existence is a delicate issue as we have explained in [1] for the stationary case. It is even more difficult in the transient case; therefore we do not discuss this question here.

We will now define four optimal control problems. These differ in the objective functional and the constraints used. In all problems we denote by $Q = \Omega \times (0, T]$ the space-time domain and by $\Sigma = (\{0\} \cup \{1\}) \times (0, T]$ the corresponding boundary part.

In the formulations of the optimal control problems we prefer the strong formulation to highlight the type of equations and the soft clamped boundary conditions. In the following considerations and in the numerical calculations we use only the weak formulation.

$$\textit{Problem I} \quad \min_{u \in \mathbb{U}_{ad}} J_I(w_s) := \min_{u \in \mathbb{U}_{ad}} \int_{\Omega} w_s(x, T) dx$$

subject to

$$\begin{aligned} \Theta(u) \partial_t^2 w_s + \partial_x^2 (\Phi(u) \partial_x^2 w_s) + \Psi(u) w_s &= R f_z \\ w_s|_{\Sigma} = \partial_x^2 w_s|_{\Sigma} &= 0 \\ w_s(\cdot, 0) = \partial_t w_s(\cdot, 0) &= 0 \end{aligned} \tag{4}$$

where

$$\mathbb{U}_{ad} = \left\{ u \in \mathbb{L}^\infty(\Omega), u_a \leq u(x) \leq u_b \text{ a.e.}, \int_{\Omega} u(x) dx = C \right\},$$

and $0 < u_a < u_b$ are given. The constant $C := V_Z/(2\pi R)$ considers the constant volume of the shell V_Z . Notice that in contrast to the load f_z , the control u is independent of time. The set \mathbb{U}_{ad} is the same in all four problems.

$$\text{Problem II} \quad \min_{u \in \mathbb{U}_{ad}} J_{II}(w_o) := \min_{u \in \mathbb{U}_{ad}} \int_{\Omega} w_o(x, T) dx$$

subject to

$$\begin{aligned} \Theta(u)\partial_t^2 w_o - \partial_x(\Upsilon(u)\partial_t^2 \partial_x w_o) + \partial_x^2(\Phi(u)\partial_x^2 w_o) + \Psi(u)w_o &= R f_z \\ w_o|_{\Sigma} = \partial_x^2 w_o|_{\Sigma} &= 0 \\ w_o(\cdot, 0) = \partial_t w_o(\cdot, 0) &= 0. \end{aligned} \quad (5)$$

In the next two problems, we use a topology optimization compliance objective functional in the following settings:

$$\text{Problem III} \quad \min_{u \in \mathbb{U}_{ad}} J_{III}(w_s) := \min_{u \in \mathbb{U}_{ad}} \iint_Q f_z w_s dx dt$$

subject to (4) and

$$\text{Problem IV} \quad \min_{u \in \mathbb{U}_{ad}} J_{IV}(w_o) := \min_{u \in \mathbb{U}_{ad}} \iint_Q f_z w_o dx dt$$

subject to (5).

These problems are similar to each other, and we refer hereafter only to the differences. Additionally, the first two objective functional, we assume $w_i(\cdot, T), i \in \{o, s\}$ greater than zero and the last two objective function is weighted by the applied force f_z . In regular situations, we can assume that the resulting deformations $w_i, i \in \{o, s\}$, have the same direction as the applied force. Then the objective functional is positive. The thickness $u = u(x)$ is the control function that influences the displacement (deflection) $w_i = w_i(x, t)$, for a given force $f_z = f_z(x, t)$.

Next, we transform these problems to nonlinear optimization problems in a Banach space. For this, we define the control-to-state operators

$$G_i : u \mapsto w_i(\cdot, T), G_i : \mathbb{L}^\infty(\Omega) \rightarrow \mathbb{V}, i \in \{o, s\}.$$

The terminal states $w_i(\cdot, T)$ are the solutions of the constraints in the weak formulations. These operators G_i are of a fairly complex type, they contain the map $u \mapsto w_i$, an linear observation operators $E_{iT} : w_i \mapsto w_i(\cdot, T)$. For the problems III and IV, we also define the mappings

$$F_i : u \mapsto w_i, F_i : \mathbb{L}^\infty(\Omega) \rightarrow \mathbb{W}_i(0, T), i \in \{o, s\}.$$

This allows us to eliminate the state w_i in the objective functionals. Let us define four reduced functionals by

$$\begin{aligned} f_I(u) &:= \int_{\Omega} G_s(u) dx & f_{II}(u) &:= \int_{\Omega} G_o(u) dx & (6) \\ f_{III}(u) &:= \iint_Q f_z F_s(u) dx dt & f_{IV}(u) &:= \iint_Q f_z F_o(u) dx dt. \end{aligned}$$

In this way, we obtain the following reduced optimal control problems:

$$\text{Problem } (P_i): \quad \min_{u \in \mathbb{U}_{ad}} f_i(u), \quad i \in \{I, II, III, IV\}.$$

Let us now formulate the first order necessary conditions of these problems. Notice all f_i are continuously Fréchet-differentiability.

Lemma 3.1. *Let $\bar{u} \in \mathbb{U}_{ad}$ be a solution of problems P_i (6). Then the variational inequality*

$$f'_i(\bar{u})(u - \bar{u}) \geq 0 \quad \forall u \in \mathbb{U}_{ad} \quad (7)$$

is fulfilled.

We refer, for instance, to [14] for the proof of this standard result. By the chain rule, we find for any $h \in \mathbb{L}^{\infty}(\Omega)$

$$\begin{aligned} f'_I(u)h &:= \int_{\Omega} G'_s(u)h dx & f'_{II}(u)h &:= \int_{\Omega} G'_o(u)h dx \\ f'_{III}(u)h &:= \iint_Q f_z F'_s(u)h dx dt & f'_{IV}(u)h &:= \iint_Q f_z F'_o(u)h dx dt \end{aligned}$$

as the derivatives of the reduced functionals. By associated adjoint equation, we can transform (7) to a computationally more comment form.

3.1 Optimality Conditions for Problem I

First we consider the optimal control problem (P_I) with simplified constraint. Here, we assume that $w_s(0), \partial_t w_s(0) \in \mathbb{V}$ and force $f_z \in \mathbb{H}^2(0, T; \mathbb{L}^2(\Omega))$. Hence, the data have higher regularity such that it follows $w_s \in \mathbb{H}^2(0, T; \mathbb{V})$ for the solution. The derivative of the control-to-state operator G_s yields a solution of an initial-boundary value problem.

Theorem 3.1. *Let the solution of simplified problem have higher regularity, $w_s \in \mathbb{H}^2(0, T; \mathbb{V})$. Then the control-to-state operator G_s is continuous Fréchet-differentiable from $\mathbb{L}^{\infty}(\Omega)$ to \mathbb{V} and it holds for any $h \in \mathbb{L}^{\infty}(\Omega)$ that*

$$G'_s(\bar{u})h = y_s(\cdot, T),$$

where $y_s \in \mathbb{H}_s^1(0, T; \mathbb{V})$ is the weak solution of the initial-boundary value problem

$$\begin{aligned} \Theta(\bar{u})\partial_t^2 y_s + \partial_x^2(\Phi(\bar{u})\partial_x^2 y_s) + \Psi(\bar{u})y_s \\ = -\Theta'(\bar{u})h\partial_t^2 \bar{w}_s - \partial_x^2(\Phi'(\bar{u})h\partial_x^2 \bar{w}_s) - \Psi'(\bar{u})h\bar{w}_s \end{aligned}$$

with boundary conditions $y_s|_{\Sigma} = \partial_x^2 y_s|_{\Sigma} = 0$ and initial data $y_s(\cdot, 0) = 0$ and $\partial_t y_s(\cdot, 0) = 0$. The functions \bar{u} and $\bar{w}_s \in \mathbb{H}_s^2(0, T; \mathbb{V})$ are a given control and the associated state of P_I , respectively.

Proof. Let $\tilde{w}_s = G_s(\bar{u}) = \bar{w}_s(\cdot, T)$ be the terminal state of the weak solution of the initial-boundary value problem

$$\begin{aligned}\Theta(\bar{u})\partial_t^2\bar{w}_s + \partial_x^2\left(\Phi(\bar{u})\partial_x^2\bar{w}_s\right) + \Psi(\bar{u})\bar{w}_s &= Rf_z \\ \bar{w}_s|_\Sigma &= \partial_x^2\bar{w}_s|_\Sigma = 0 \\ \bar{w}_s(\cdot, 0) &= \partial_t\bar{w}_s(\cdot, 0) = 0\end{aligned}$$

and let $\tilde{w}_u = w_u(\cdot, T) = G_s(\bar{u} + h)$, $h \in \mathbb{L}^\infty(\Omega)$, be the terminal state of the weak solution of the initial-boundary value problem

$$\begin{aligned}\Theta(\bar{u} + h)\partial_t^2w_u + \partial_x^2\left(\Phi(\bar{u} + h)\partial_x^2w_u\right) + \Psi(\bar{u} + h)w_u &= Rf_z \\ w_u|_\Sigma &= \partial_x^2w_u|_\Sigma = 0 \\ w_u(\cdot, 0) &= \partial_tw_u(\cdot, 0) = 0.\end{aligned}$$

We consider the difference $G_s(\bar{u} + h) - G_s(\bar{u})$, which is the difference of the terminal values of w_s and w_u . The terminal values $\bar{w}_s(\cdot, T)$ and $w_u(\cdot, T)$ assigned by the linear observation operator E_{sT} clearly are the solutions $\bar{w}_s(\cdot, \cdot)$ and $w_u(\cdot, \cdot)$. We can subtract the initial-boundary value problems and invoke the Fréchet-differentiability of the Nemytskij operators:

$$\begin{aligned}\Theta(\bar{u} + h)\partial_t^2(w_u - \bar{w}_s) + [\Theta'(\bar{u})h + r_\Theta(\bar{u}, h)]\partial_t^2\bar{w}_s \\ + \partial_x^2[\Phi(\bar{u} + h)\partial_x^2(w_u - \bar{w}_s)] + \partial_x^2([\Phi'(\bar{u})h + r_\Phi(\bar{u}, h)]\partial_x^2\bar{w}_s) \\ + \Psi(\bar{u} + h)(w_u - \bar{w}_s) + [\Psi'(\bar{u})h + r_\Psi(\bar{u}, h)]\bar{w}_s = 0.\end{aligned}$$

The initial data and boundary conditions remain unchanged.

We put $w_u - \bar{w}_s = y_s + y_r$ and analogous expression holds for the terminal values $\tilde{w}_u - \tilde{w}_s = \tilde{y}_s + \tilde{y}_r$ and $\tilde{y}_s = y_s(\cdot, T)$ by use E_{sT} . Let y_s be the weak solution of the initial-boundary value problem

$$\begin{aligned}\Theta(\bar{u})\partial_t^2y_s + \partial_x^2\left(\Phi(\bar{u})\partial_x^2y_s\right) + \Psi(\bar{u})y_s \\ = -\Theta'(\bar{u})h\partial_t^2\bar{w}_s - \partial_x^2\left(\Phi'(\bar{u})h\partial_x^2\bar{w}_s\right) - \Psi'(\bar{u})h\bar{w}_s \\ y_s|_\Sigma = \partial_x^2y_s|_\Sigma = 0 \\ y_s(\cdot, 0) = \partial_t y_s(\cdot, 0) = 0.\end{aligned}$$

We take the difference $y_r = w_u - \bar{w}_s - y_s$ to determine an equation for y_r and use the Fréchet-differentiability of the Nemytskij operators:

$$\begin{aligned}\Theta(\bar{u} + h)\partial_t^2y_r + \partial_x^2(\Phi(\bar{u} + h)\partial_x^2y_r) + \Psi(\bar{u} + h)y_r + [\Theta'(\bar{u})h + r_\Theta(\bar{u}, h)]\partial_t^2y_s \\ + r_\Theta(\bar{u}, h)\partial_t^2\bar{w}_s + \partial_x^2([\Phi'(\bar{u})h + r_\Theta(\bar{u}, h)]\partial_x^2y_s) + [\Psi'(\bar{u})h + r_\Psi(\bar{u}, h)]y_s \\ + \partial_x^2(r_\Phi(\bar{u}, h)\partial_x^2\bar{w}_s) + r_\Psi(\bar{u}, h)\bar{w}_s = 0,\end{aligned}$$

where $\tilde{y}_r = y_r(\cdot, T)$ satisfied the needed properties of a remainder term. The initial data and boundary conditions of the equations for y_s and y_r are analogous to the equations for \bar{w}_s and w_u .

Next, we transform the initial-boundary value problem for y_s into the complete variational formulation and discuss the existence of a weak solution,

$$\begin{aligned} & \iint_Q \{\Theta(\bar{u})\partial_t^2 y_s v + \Phi(\bar{u})\partial_x^2 y_s \partial_x^2 v + \Psi(\bar{u})y_s v\} dx dt \\ &= \iint_Q \{-\Theta'(\bar{u})\partial_t^2 \bar{w}_s v - \Phi'(\bar{u})\partial_x^2 \bar{w}_s \partial_x^2 v - \Psi'(\bar{u})\bar{w}_s v\} h dx dt \end{aligned}$$

for each $v \in \mathbb{W}_s(0, T)$. We define

$$f_{y_s}(v) := \iint_Q \{-\Theta'(\bar{u})\partial_t^2 \bar{w}_s v - \Phi'(\bar{u})\partial_x^2 \bar{w}_s \partial_x^2 v - \Psi'(\bar{u})\bar{w}_s v\} h dx dt$$

and $\Sigma(u)(x) := \max\{|\Theta'(\bar{u})|, |\Phi'(\bar{u})|, |\Psi'(\bar{u})|\}$. Then it follows

$$\|f_{y_s}\| \leq \tilde{C} \|\Sigma(u)\|_{\mathbb{L}^\infty} \|h\|_{\mathbb{L}^\infty} \|\bar{w}_s\|_{\mathbb{H}^2(0, T; \mathbb{V})}.$$

Since the functions on the right hand side are obviously square integrable, $f_{y_s}(v)$ is also square integrable, we can apply the existence theorem 2.2. For the solution y_s , it follows the estimate,

$$\|\mathbf{y}_s\|_{\mathbb{W}_s^2(0, T)} \leq C \|\Sigma\|_{\mathbb{L}^\infty} \|h\|_{\mathbb{L}^\infty} \|f_z\|_{\mathbb{L}^2(0, T; \mathbb{H})},$$

with constant C . From the assumption on higher regularity of the solution y_s , it follows $y_s \in \mathbb{H}^1(0, T; \mathbb{V})$ and $\partial_t^2 y_s \in \mathbb{L}^2(0, T; \mathbb{L}^2(\Omega))$. We will need this property of higher regularity with respect to y_s below.

We turn to the equation for the remainder y_r . In order to calculate a complete variational formulation, we discuss the existence of a solution of

$$\begin{aligned} & \iint_Q \{\Theta(\bar{u} + h)\partial_t^2 y_r v + \Phi(\bar{u} + h)\partial_x^2 y_r \partial_x^2 v + \Psi(\bar{u} + h)y_r v\} dx dt \\ &= \iint_Q \{[\Theta'(u)h + r_\Theta(\bar{u}, h)]\partial_t^2 y_s v + r_\Theta(\bar{u}, h)\partial_t^2 \bar{w}_s v \\ &+ [\Phi'(\bar{u})h + r_\Theta(\bar{u}, h)]\partial_x^2 y_s \partial_x^2 v + [\Psi'(\bar{u})h + r_\Psi(\bar{u}, h)]y_s v \\ &+ r_\Phi(\bar{u}, h)\partial_x^2 \bar{w}_s \partial_x^2 v + r_\Psi(\bar{u}, h)\bar{w}_s v\} dx dt, \end{aligned}$$

for each $v \in \mathbb{W}_s(0, T)$. For the estimate the solution y_r , we define

$$\begin{aligned} f_{y_r}(v) &:= \iint_Q \{[\Theta'(u)h + r_\Theta(\bar{u}, h)]\partial_t^2 y_s v + r_\Theta(\bar{u}, h)\partial_t^2 \bar{w}_s v \\ &+ [\Phi'(\bar{u})h + r_\Theta(\bar{u}, h)]\partial_x^2 y_s \partial_x^2 v + [\Psi'(\bar{u})h + r_\Psi(\bar{u}, h)]y_s v \\ &+ r_\Phi(\bar{u}, h)\partial_x^2 \bar{w}_s \partial_x^2 v + r_\Psi(\bar{u}, h)\bar{w}_s v\} dx dt, \end{aligned}$$

and $r_{y_r}(\bar{u}, h)(x) := \max\{|r_\Theta(\bar{u}, h)(x)|, |r_\Phi(\bar{u}, h)(x)|, |r_\Psi(\bar{u}, h)(x)|\}$. Obviously, every function of the right side is square integrable. For the norm of the functional f_{y_r} , we calculate for all $v \in \mathbb{W}_s^2(0, T)$:

$$\begin{aligned} \|f_{y_r}\| &\leq C \left\{ \|\Sigma\|_{\mathbb{L}^\infty}^2 \|h\|_{\mathbb{L}^\infty}^2 + \|r_{y_r}(\bar{u}, h)\|_{\mathbb{L}^\infty} \|\Sigma\|_{\mathbb{L}^\infty} \|h\|_{\mathbb{L}^\infty} \right. \\ &\quad \left. + \|r_{y_r}(\bar{u}, h)\|_{\mathbb{L}^\infty} \right\} \|f_z\|_{\mathbb{L}^2(0, T; \mathbb{H})}. \end{aligned}$$

Now we apply the existence theorem 2.2 to the solution y_r to obtain the estimate

$$\begin{aligned} \|\mathbf{y}_r\|_{\mathbb{W}_s^2(0,T)} \leq C \left\{ \|\Sigma\|_{\mathbb{L}^\infty}^2 \|h\|_{\mathbb{L}^\infty}^2 + \|r_{y_r}(\bar{u}, h)\|_{\mathbb{L}^\infty} \|\Sigma\|_{\mathbb{L}^\infty} \|h\|_{\mathbb{L}^\infty} \right. \\ \left. + \|r_{y_r}(\bar{u}, h)\|_{\mathbb{L}^\infty} \right\} \|f_z\|_{\mathbb{L}^2(0,T;\mathbb{H})}, \end{aligned}$$

with some constant C .

The solution y_s of the initial-boundary value problem is linear with respect to $h \in \mathbb{L}^\infty(\Omega)$, and the linear observation operator E_{sT} does not change this property. We have to show the remainder property of the solution y_r . We divide remainder term by the norm of h , and have to show that for $h \rightarrow 0$ this fractions tends to zero:

$$\begin{aligned} \frac{\|\mathbf{y}_r\|_{\mathbb{W}_s^2(0,T)}}{\|h\|_{\mathbb{L}^\infty}} \leq C \left\{ \|\Sigma\|_{\mathbb{L}^\infty}^2 \|h\|_{\mathbb{L}^\infty} + \|r_{y_r}(\bar{u}, h)\|_{\mathbb{L}^\infty} \|\Sigma\|_{\mathbb{L}^\infty} \right. \\ \left. + \frac{\|r_{y_r}(\bar{u}, h)\|_{\mathbb{L}^\infty}}{\|h\|_{\mathbb{L}^\infty}} \right\} \|f_z\|_{\mathbb{L}^2(0,T;\mathbb{H})}. \end{aligned}$$

The term $\|\Sigma\|_{\mathbb{L}^\infty}^2 \|h\|_{\mathbb{L}^\infty}$ tends obviously to zero as $h \rightarrow 0$. For $r_{y_r}(\bar{u}, h)$, we use the remainder property of the Nemytskij operators. The conclusion is that $y_r \rightarrow 0$ for $h \rightarrow 0$. After applying the linear observation operator E_{sT} it follows $\tilde{y}_r \rightarrow 0$, too. Since $\tilde{y}_r \in \mathbb{V}$, the remainder property is valid with respect to the space \mathbb{V} and thus the assertion of the proposition follows. \square

Next, we are able to formulate the first order necessary conditions in a more convenient form. To this aim, we define the adjoint state p_I .

Definition 3.1. *The adjoint state $p_I \in \mathbb{W}_s(0, T)$ associated with \bar{u} is the weak solution of the final-time-boundary value problem*

$$\begin{aligned} \Theta(\bar{u})\partial_t^2 p_I + \partial_x^2 \left(\Phi(\bar{u})\partial_x^2 p_I \right) + \Psi(\bar{u})p_I &= 0 \\ p_I|_\Sigma = \partial_x^2 p_I|_\Sigma &= 0 \\ p_I(\cdot, T) = 0, \quad \Theta(\bar{u})\partial_t p_I(\cdot, T) &= -1. \end{aligned} \tag{8}$$

For this problem the existence of a solution has been proved, in [11]. The functions p_i , $i \in \{I, II, III, IV\}$ can be interpreted as Lagrange multipliers associated with the original or simplified equations.

Lemma 3.2. *Let functions $\bar{u}, h \in \mathbb{L}^\infty(\Omega)$ be given.*

Furthermore, let $\mathbf{y}_s \in \mathbb{H}^1(0, T; \mathbb{V})$ be the weak solution of

$$\begin{aligned} \Theta(\bar{u})\partial_t^2 y_s + \partial_x^2 \left(\Phi(\bar{u})\partial_x^2 y_s \right) + \Psi(\bar{u})y_s \\ = -\Theta'(\bar{u})h\partial_t^2 \bar{w}_s - \partial_x^2 \left(\Phi'(\bar{u})h\partial_x^2 \bar{w}_s \right) - \Psi'(\bar{u})h\bar{w}_s \\ y_s|_\Sigma = \partial_x^2 y_s|_\Sigma = 0 \\ y_s(\cdot, 0) = \partial_t y_s(\cdot, 0) = 0 \end{aligned}$$

and let $\mathbf{p}_I \in \mathbb{H}^1(0, T; \mathbb{V})$ be the weak solution of

$$\begin{aligned}\Theta(\bar{u})\partial_t^2 p_I + \partial_x^2 \left(\Phi(\bar{u})\partial_x^2 p_I \right) + \Psi(\bar{u})p_I &= 0 \\ p_I|_\Sigma &= \partial_x^2 p_I|_\Sigma = 0 \\ p_I(\cdot, T) &= 0 \quad \Theta(\bar{u})\partial_t p_I(\cdot, T) = -1.\end{aligned}$$

Then it holds

$$\int_{\Omega} y_s(x, T) dx = \iint_Q \left\{ \Theta'(\bar{u})\partial_t \bar{w}_s \partial_t p_I - \Phi'(\bar{u})\partial_x^2 \bar{w}_s \partial_x^2 p_I - \Psi'(\bar{u})\bar{w}_s p_I \right\} h dx dt.$$

The proof of this lemma is simple and omitted here. With this lemma, we can formulate necessary optimality conditions.

Corollary 3.1 (Necessary condition for Problem I). *Any optimal control \bar{u} and the corresponding optimal final state $\bar{w}_s(\cdot, T) = G_s(\bar{u})$ for (P_I) must fulfill the variational inequality*

$$\iint_Q \left\{ \Theta'(\bar{u})\partial_t \bar{w}_s \partial_t p_I - \Phi'(\bar{u})\partial_x^2 \bar{w}_s \partial_x^2 p_I - \Psi'(\bar{u})\bar{w}_s p_I \right\} (u - \bar{u}) dx dt \geq 0$$

for each $u \in \mathbb{U}_{ad}$, where the Lagrange multiplier $p_I \in \mathbb{W}_s(0, T)$ is the adjoint state defined by (8).

3.2 Optimality Conditions for Problem II-IV

In the same way as in the preceding section, we obtain necessary conditions for the problem II-IV. In view of the analogy, we only formulate the associated adjoint equations and variational inequalities.

Problem II

$$\begin{aligned}\Theta(\bar{u})\partial_t^2 p_{II} - \partial_x(\Upsilon(\bar{u})\partial_t^2 \partial_x p_{II}) + \partial_x^2 \left(\Phi(\bar{u})\partial_x^2 p_{II} \right) + \Psi(\bar{u})p_{II} &= 0 \\ p_{II}|_\Sigma &= \partial_x^2 p_{II} = 0 \\ \Theta(\bar{u})p_{II}(\cdot, T) - \partial_x(\Upsilon(\bar{u})\partial_x p_{II}(\cdot, T)) &= 0 \\ 1 + \Theta(\bar{u})\partial_t p_{II}(\cdot, T) - \partial_x(\Upsilon(\bar{u})\partial_t \partial_x p_{II}(\cdot, T)) &= 0 \\ \iint_Q \left\{ -\Theta'(\bar{u})\partial_t^2 \bar{w}_o p_{II} - \Upsilon'(\bar{u})\partial_t^2 \partial_x \bar{w}_o \partial_x p_{II} - \Phi'(\bar{u})\partial_x^2 \bar{w}_o \partial_x^2 p_{II} \right. \\ &\quad \left. - \Psi'(\bar{u})\bar{w}_o p_{II} \right\} (u - \bar{u}) dx dt \geq 0\end{aligned}$$

for each $u \in \mathbb{U}_{ad}$.

Problem III

$$\begin{aligned}\Theta(\bar{u})\partial_t^2 p_{III} + \partial_x^2 \left(\Phi(\bar{u})\partial_x^2 p_{III} \right) + \Psi(\bar{u})p_{III} &= f_z \\ p_s|_\Sigma &= \partial_x^2 p_{III}|_\Sigma = 0 \\ p_{III}(\cdot, T) &= \partial_t p_{III}(\cdot, T) = 0 \\ \iint_Q \left\{ \Theta'(\bar{u})\partial_t \bar{w}_s \partial_t p_{III} - \Phi'(\bar{u})\partial_x^2 \bar{w}_s \partial_x^2 p_{III} - \Psi'(\bar{u})\bar{w}_s p_{III} \right\} (u - \bar{u}) dx dt &\geq 0\end{aligned}$$

for each $u \in \mathbb{U}_{ad}$.

Problem IV

$$\begin{aligned} \Theta(\bar{u})\partial_t^2 p_{IV} - \partial_x(\Upsilon(\bar{u})\partial_t^2 \partial_x p_{IV}) + \partial_x^2(\Phi(\bar{u})\partial_x^2 p_{IV}) + \Psi(\bar{u})p_{IV} &= f_z \\ p_{IV}|_{\Sigma} = \partial_x^2 p_{IV} &= 0 \\ p_{IV}(\cdot, T) = \partial_t p_{IV}(\cdot, T) &= 0 \\ \iint_Q \left\{ -\Theta'(\bar{u})\partial_t^2 \bar{w}_o p_{IV} - \Upsilon'(\bar{u})\partial_t^2 \partial_x \bar{w}_o \partial_x p_{IV} - \Phi'(\bar{u})\partial_x^2 \bar{w}_o \partial_x^2 p_{IV} \right. \\ \left. - \Psi'(\bar{u})\bar{w}_o p_{IV} \right\} (u - \bar{u}) dx dt &\geq 0 \end{aligned}$$

for each $u \in \mathbb{U}_{ad}$.

4 Numerical Implementation and Solution of the Problems

The constraints are hyperbolic partial differential equation of fourth order with respect to the spatial variables and of second order in time. We solve these equations by transforming them into a system of parabolic partial differential equations that can be solved by the finite element method in combination with Rothe's method. We use σ -weighted difference schemes for the time derivatives and apply the finite element method in x . For the resulting optimal control problem we use the optimization code *fmincon* that is part of the software-package MATLAB. Subsequently, we give some details to the finite element method (FEM) [8,11,15] that is used to determine approximate solutions of the equations and the associated adjoint equations. The starting point of this method are the variational formulations (2) and (3).

In order to approximate the solution space \mathbb{V} , we use Hermite interpolation of the functions w_i , $i \in \{o, s\}$ and p_i with step size parameter h . First, we define the discrete solution space

$$V_h = \left\{ w_h(\cdot) : w_h(\cdot) = \sum_{j=0}^n w_j^0 p_j(\cdot) + w_j^1 q_j(\cdot) \right\} \subset V.$$

In this definition of the solution space, conformal finite elements are included. Next, we define for each time step $t_m \in (0, T]$:

$$w_{ih}^m(\cdot, t_m) = \sum_{j=0}^n w_{ij}^0(t_m) p_j(\cdot) + w_{ij}^1(t_m) q_j(\cdot) \quad w_{ih}^m \in \mathbb{V}_h$$

with basis functions $p_j, q_j \in \mathcal{P}_3(\Omega)$ for $j = 0, 1, \dots, n$ (cubic polynomials), where n is the number of grid points. The $w_{ij}^0(t_m), w_{ij}^1(t_m)$, $i \in \{o, s\}$, are certain real node parameters. For the node parameters, we have in mind

$$w_{ij}^0(t_m) \approx w_{ih}(x_j, t_m) \text{ and } w_{ij}^1(t_m) \approx \partial_x w_{ih}(x_j, t_m).$$

Furthermore, we define discrete bilinear forms and a linear form

$$\begin{aligned} a_h(w_h, v_h, t_m) &:= \int_{\Omega} \Phi(u_h) d_x^2 w_h(t_m) d_x^2 v_h + \Psi(u_h) w_h(t_m) v_h \, dx, \\ g_h(w_h, v_h, t_m) &:= \int_{\Omega} \Upsilon(u_h) d_x w_h(t_m) d_x v_h + \Psi(u_h) w_h(t_m) v_h \, dx, \\ F_h(v_h, t_m) &:= R \int_{\Omega} f_z(t_m) v_h \, dx. \end{aligned}$$

For equations or adjoint equations (with small modifications in the linear form), we define the following discrete problems:

Find $w_{ih} \in V_h$, $i \in \{o, s\}$ solving

$$\begin{aligned} (\Theta(u_h) \ddot{w}_{oh}^m, v_h)_{\mathbb{L}^2} + g_h(w_{oh}^m, v_h, t_m) + a_h(w_{oh}^m, v_h, t_m) &= F_h(v_h) \quad \text{or} \\ (\Theta(u_h) \ddot{w}_{sh}^m, v_h)_{\mathbb{L}^2} + a_h(w_{sh}^m, v_h, t_m) &= F_h(v_h) \quad \forall v_h \in V_h \end{aligned}$$

for each time step $t_m \in (0, T]$ and given initial data. Analogously we discretize the adjoint equations. Now we set $y_{ih}^m = \dot{w}_{ih}^m$ and it follows

$$\begin{aligned} (\dot{w}_{oh}^m - y_{oh}^m, v_h)_{\mathbb{L}^2} &= 0 \\ (\Theta(u_h) \dot{y}_{oh}^m, v_h)_{\mathbb{L}^2} + g_h(w_{oh}^m, v_h, t_m) + a_h(w_{oh}^m, v_h, t_m) &= F_h(v_h) \quad \text{or} \\ (\dot{w}_{sh}^m - y_{sh}^m, v_h)_{\mathbb{L}^2} &= 0 \\ (\Theta(u_h) \dot{y}_{sh}^m, v_h)_{\mathbb{L}^2} + a_h(w_{sh}^m, v_h, t_m) &= F_h(v_h) \quad \forall v_h \in V_h \end{aligned}$$

To solve the discrete problems, we can apply standard techniques of linear algebra. The control function u is discretized by piecewise linear interpolation,

$$u_h = \sum_{j=0}^n u_j l_j$$

with linear continuous basis functions l_j ; hence it holds $u_h \in \mathcal{C}(\overline{\Omega})$. Therefore, we have established an isomorphism

$$u_h \iff \vec{u}_h = [u_0, \dots, u_n] \in \mathbb{R}^{n+1}$$

and the objective functionals

$$\begin{aligned} f_{Ih}(u_h) &= \int_{\Omega} w_{sh}^m(\cdot, T) \, dx & f_{IIh}(u_h) &= \int_{\Omega} w_{oh}^m(\cdot, T) \, dx \\ f_{IIIh}(u_h) &= \iint_Q f_z w_{sh}^m \, dx \, dt & f_{IV}(u_h) &= \iint_Q f_z w_{oh}^m \, dx \, dt \end{aligned}$$

can be expressed by mappings $\varphi_i : \mathbb{R}^{n+1} \rightarrow \mathbb{R}$, $i \in \{I, II, III, IV\}$:

$$\varphi_{ih} : \vec{u}_h \mapsto u_h \mapsto f_{ih}(u_h).$$

These functions will be used in the numerical implementations. The optimal control problems are finally approximated by

$$\min_{\vec{u} \in \mathbb{U}_{ad}^h} \varphi_{ih}(\vec{u}_h),$$

where the set \mathbb{U}_{ad}^h will be defined later.

4.1 Implementation of the Derivative of the Objective Functional

The optimization solver *fmincon* calculates the discrete derivative $\nabla\varphi_{ih}(\vec{u}_h)$ by finite differences. This means that, in principle, our adjoint calculus is not needed by *fmincon*. However, proceeding in this way, the computing times will be very long. The tool *fmincon* can be accelerated by providing information on the derivative. During the analytical treatment of the optimal control problem, we determined the derivative $f'_i(u)$.

Numerically, we implement this derivative by FEM to compute $\nabla\varphi_{ih}(\vec{u}_h)$. During the numerical optimization process, this gradient is passed to the solver *fmincon*. This reduces the running time of the optimization algorithm considerably. On the other hand, this approach might be problematic, because we approximate $\nabla\varphi_{ih}$ by means of a discretized continuous adjoint equation. This is not necessarily equal to the exact discrete gradient $\nabla\varphi_{ih}$. The solver *fmincon* is testing the quality of the transmitted gradient $\nabla\varphi_{ih}$ by finite differences.

During our numerical experiments, it turned out that the difference between our gradient $\nabla\varphi_{ih}$ (computed via the adjoint equation) and the "exact" discrete gradient was marginal of the order 10^{-6} for sufficiently small discretization x -parameter h and t -parameter τ for time.

We should mention that the computation of the gradient via the adjoint equation was numerically more stable than the use of the one generated by *fmincon*. Of course, the solution of the optimization problem with finite element gradients is identical with the one obtained from finite difference gradients. We used a discretized version of this gradient, where we consider arbitrary directions $z_h \in \mathcal{C}(\bar{\Omega})$ (the analog approach to u).

For the function $w_i, p_i, i \in \{I, II, III, IV\}$, we apply the two-dimensional Hermite interpolation:

$$\tilde{w}_{ih}^\tau(x, t) = \sum_{j=0}^m \sum_{i=0}^n \sum_{a,b=0}^1 \hat{\alpha}_{ij}^{ab} s_i^a(x) s_j^b(t)$$

with global functions $s_i, s_j \in \mathcal{P}_3$ (cubic polynomials) and τ the time-stepsize. The parameters a, b denote the derivative $\frac{d^a}{dx^a}, \frac{d^b}{dt^b}$ of the function s , and the node parameters $\hat{\alpha}_{ij}^{ab}$ are the derivatives of the functions w_i or p_i at the grid point

$$\hat{\alpha}_{ij}^{00} = w_i(x_i, t_j) \quad \hat{\alpha}_{ij}^{10} = \partial_x w_i(x_i, t_j) \quad \hat{\alpha}_{ij}^{01} = \partial_t w_i(x_i, t_j) \quad \hat{\alpha}_{ij}^{11} = \partial_x \partial_t w_i(x_i, t_j)$$

This approach involves the approximation of the space \mathbb{V} . Through this approach, practically the Bogner-Fox-Schmidt element is used. With these conventions we obtain for $\alpha \in \{I, III\}$:

$$\begin{aligned} \nabla f_{\alpha h}(u_h) z_h = & \iint_Q \left\{ \Theta'(u_h) \partial_t \tilde{w}_{\alpha h}^m \partial_t \tilde{p}_{\alpha h}^m - \Phi'(u_h) \partial_x^2 \tilde{w}_{\alpha h}^m \partial_x^2 \tilde{p}_{\alpha h}^m \right. \\ & \left. - \Psi'(u_h) \tilde{w}_{\alpha h}^m \tilde{p}_{\alpha h}^m \right\} z_h \, dx \, dt \end{aligned}$$

and for $\beta \in \{II, IV\}$:

$$\begin{aligned} \nabla f_{\beta h}(u_h)z_h = & \iint_Q \left\{ \Theta'(u_h)\partial_t \tilde{w}_{\beta h}^m \partial_t \tilde{p}_{\beta h}^m + \Upsilon'(u_h)\partial_t \partial_x \tilde{w}_{\beta h}^m \partial_t \partial_x \tilde{p}_{\beta h}^m \right. \\ & \left. - \Phi'(u_h)\partial_x^2 \tilde{w}_{\beta h}^m \partial_x^2 \tilde{p}_{\beta h}^m - \Psi'(u_h)\tilde{w}_{\beta h}^m \tilde{p}_{\beta h}^m \right\} z_h \, dx \, dt, \end{aligned}$$

for each z_h . For any direction z_h , we can choose the nodal basis functions l_j successively for $j = 0, \dots, n$. It follows for the numerical implementation of the discrete gradient vector that

$$\begin{aligned} [\nabla \varphi_{\alpha h}]_j = & \sum_{i=1}^n \int_{E^{(i)}} \int_0^T \left\{ \Theta'(u_h)\partial_t \tilde{w}_{\alpha h}^m \partial_t \tilde{p}_{\alpha h}^m - \Phi'(u_h)\partial_x^2 \tilde{w}_{\alpha h}^m \partial_x^2 \tilde{p}_{\alpha h}^m \right. \\ & \left. - \Psi'(u_h)\tilde{w}_{\alpha h}^m \tilde{p}_{\alpha h}^m \right\} dt \, l_j \, dx \end{aligned}$$

and

$$\begin{aligned} [\nabla \varphi_{\beta h}]_j = & \sum_{i=1}^n \int_{E^{(i)}} \int_0^T \left\{ \Theta'(u_h)\partial_t \tilde{w}_{\beta h}^m \partial_t \tilde{p}_{\beta h}^m + \Upsilon'(u_h)\partial_t \partial_x \tilde{w}_{\beta h}^m \partial_t \partial_x \tilde{p}_{\beta h}^m \right. \\ & \left. - \Phi'(u_h)\partial_x^2 \tilde{w}_{\beta h}^m \partial_x^2 \tilde{p}_{\beta h}^m - \Psi'(u_h)\tilde{w}_{\beta h}^m \tilde{p}_{\beta h}^m \right\} dt \, l_j \, dx \end{aligned}$$

for $j = 0, \dots, n$. The same implementation is used for checking the first order necessary optimality conditions, see Section 3.1 – 3.4.

4.2 Numerical Solution of the Optimization Problem

The reduced problems (6) are our starting point for the direct solution of the optimal control problems. We solve the finite dimensional optimization problems

$$\min_{\vec{u}_h \in \mathbb{U}_h^{ad}} \varphi_{ih}(\vec{u}_h) \quad i \in \{I, II, III, IV\} \quad (9)$$

subject to

$$A_h \vec{u}_h = C, \quad (10)$$

where

$$\mathbb{U}_h^{ad} = \{\vec{u}_h \in \mathbb{R}^{n+1} \mid \vec{u}_a \leq \vec{u}_h \leq \vec{u}_b\}$$

and

$$A_h = \begin{bmatrix} \frac{h}{2} & h & \dots & h & \frac{h}{2} \end{bmatrix} \in \mathbb{R}^{n+1}.$$

The volume condition (10) is formulated as an additional constraint. It was derived by the trapezoidal rule. The constant C (volume) depends on the particular problem. The restrictions on \vec{u}_h are defined componentwise.

The tool *fmincon* of the MATLAB (optimization toolbox) is designed for solving optimization problems with linear (or nonlinear) objective functions and linear (or nonlinear) constraints, both in form of equations as well as inequalities. The routine *fmincon* requires the following inputs: the values of the discrete objective functional $\varphi_{ih}(\vec{u}_h)$, the volume condition (10) by input of A_h

and C , the vectors \vec{u}_a, \vec{u}_b , and the discrete gradient vector $\nabla\varphi_{ih}$ that leads to a reduction of running time. The program stops, if changes of the objective functional are smaller than a prescribed threshold, the violations of the constraint be located within the tolerances, and the necessary conditions for the optimality of the solution are fulfilled. The output is the optimal solution vector \vec{u}_h , the discrete Lagrange multiplier q_h for the volume condition, and the Lagrange multipliers $\vec{\mu}_a, \vec{\mu}_b$ for the control restrictions, where they are active. Whether the solution \bar{u}_h of the discrete optimal control problem really be a candidate for the optimal solution is verified by checking the first order necessary condition. Let us call this "optimality test".

The variational inequalities for problems I-IV are the starting points for evaluating the optimality of the numerically computed optimal solutions \bar{u}_h . Pointwise evaluation of the first order necessary condition, as done in [14] for optimal control problems with box constraints, is not applicable in our case due to the non-constant ansatz for the control function u and the additional volume condition. Let us define the linear forms

$$\begin{aligned} b_\alpha(z) &:= \iint_Q \{-\Theta'(\bar{u})\partial_t w_\alpha \partial_t p_\alpha + \Phi'(\bar{u})\partial_x^2 w_\alpha \partial_x^2 p_\alpha \\ &\quad + \Psi'(\bar{u})w_\alpha p_\alpha\} z \, dx \, dt \\ b_\beta(z) &:= \iint_Q \{-\Theta'(\bar{u})\partial_t w_\beta \partial_t p_\beta - \Upsilon(\bar{u})'\partial_t \partial_x w_\beta \partial_t \partial_x p_\beta \\ &\quad + \Phi'(\bar{u})\partial_x^2 w_\beta \partial_x^2 p_\beta + \Psi'(\bar{u})w_\beta p_\beta\} z \, dx \, dt. \end{aligned}$$

The variational inequalities for problems (P_i) are equivalent to

$$\max_{z \in \mathbb{U}_{ad}} b_i(z) = b_i(\bar{u}). \quad (11)$$

hence, to be optimal, \bar{u} must solve a linear continuous optimization problem. As done for the control u , we linearly interpolate the function z . We have also a correspondence

$$\psi_{ih} : \vec{z}_h \mapsto z_h \mapsto b_{ih}(z_h).$$

Hence we obtain the discrete problem:

$$\max_{\vec{z}_h \in \mathbb{U}_h^{ad}} \psi_{ih}(\vec{z}_h) \quad (12)$$

subject to (10).

A first test is performed as follows: After computing \bar{u}_h , we compute the state \tilde{w}_{ih}^τ and the adjoint state \tilde{p}_{ih}^τ . Then we solve the optimal problems (12). The solution is \bar{z}_h . If \bar{u}_h is optimal for the discretized problem, the equation $\bar{u}_h = \bar{z}_h$ should hold. In general, there is an error and the difference $\|\bar{u}_h - \bar{z}_h\|$ indicates the precision of \bar{u}_h . This procedure shows, how good \bar{u}_h solves the discretized optimization problem. Another test is used to estimate, how well \bar{u}_h solves the reduced problem.

To perform this optimality test, the problem (12) is also solved by the optimization solver *fmincon*. The gradient $\nabla\psi_{ih}$ is calculated by finite elements and is passed to *fmincon*. We used $\vec{z}_0 = \bar{u}_h + \epsilon \cdot \mathbf{1}$ as starting approximation

for our examples below. The parameter $\epsilon \in \mathbb{R}$ generates a perturbation in all components of optimal solution \bar{u}_h of (9). The output is the optimal solution \bar{z}_h of (11).

5 Examples

Let us discuss some test examples. They are used to evaluate the quality of the necessary optimality conditions and demonstrate the advantage of using finite elements gradients. In the examples, we use the material parameters

$$E = 2.1 \cdot 10^2, \nu = 0.3, \rho = 7.8, R = 1$$

that is the elastic modulus E , the Poisson number ν , the density ρ and the radius R . The first three parameters depend on the material and the last parameter depends on the particular geometry. To discretize the transient problems, we choose an equidistant grid for x and t -location. For this grid, we compute the discrete optimal solution \bar{u}_h and the corresponding optimal state \bar{w}_{*h} . We set final-time $T = 1$, this is only for our academic examples.

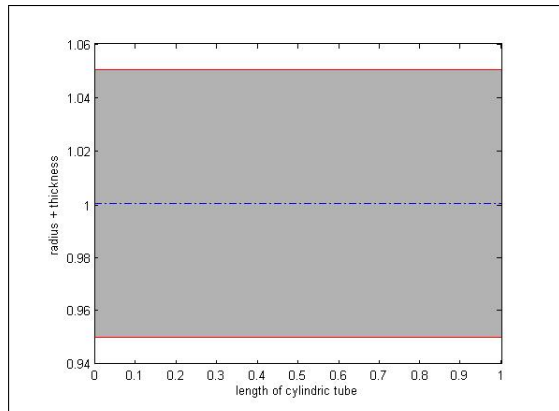


Figure 2: Starting configuration

Figure 2 shows a longitudinal cut through the cylindrical shell, where we only plot the upper part due to symmetry. The dash-dotted-line represents the central plane of the cylindrical shell. This is the starting configuration for all examples. We define the vector $\mathbf{1} \in \mathbb{R}^{n+1}$ containing the number 1 in all entries. As restrictions to the control we set the constants $u_a = 0.05 \cdot \mathbf{1}$ and $u_b = 0.15 \cdot \mathbf{1}$. The fixed volume is prescribed by $C = 0.6283$, and $u_0 = 0.1 \cdot \mathbf{1}$ is the initial value on the control. The figures below show the optimal solution \bar{u}_h , the solution \bar{z}_h of the variational inequality and the corresponding shape of the cylindrical shell for different choices of f_z .

Example 1. We take as force $f_z = x(1 - x)$.

First, we justify the use of the finite element gradient via the adjoint equation. We have chosen these figures by $\#x\text{-nodes} \times \#t\text{-nodes} := 100 \times 100$.

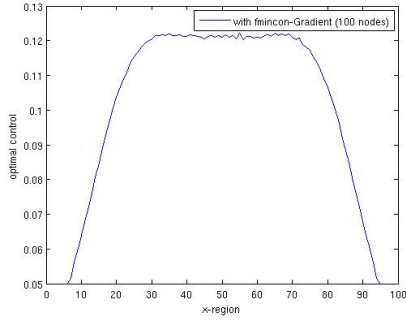


Figure 3: Optimal thickness \bar{u}_{Ih} on using the finite difference method of *fmincon* for gradients (fdm-gradient)

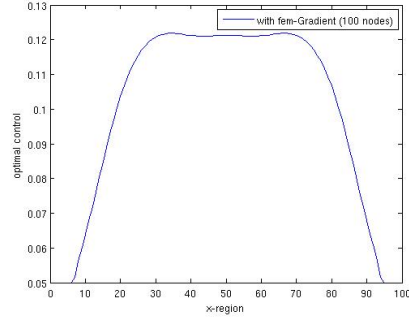


Figure 4: Optimal thickness \bar{u}_{Ih} by using the finite element method and the adjoint equation for the gradients (fem-gradient)

As can be easily seen, the use of the finite element gradient is of great advantage. The second major advantage is the acceleration of the optimization solver *fmincon* that required the following running times:

$\#x \times \#t$	<i>fmincon</i> with fdm-gradient	<i>fmincon</i> with fem-gradient
50×50	3429.59	147.941
100×100	66441.10	645.231

The values of the 2nd and 3rd column are given in seconds. These values were calculated by Problem I. The next pictures show the numerically calculated optimal control \bar{u}_{Ih} and the associated configuration of the cylindrical shell. Again, we only display its upper half.

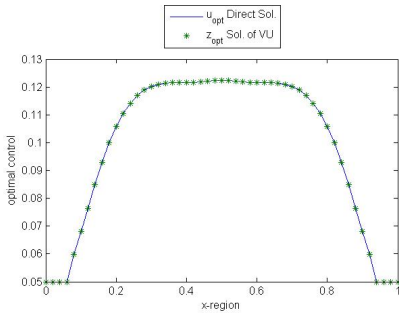


Figure 5: Optimal thickness \bar{u}_{Ih}

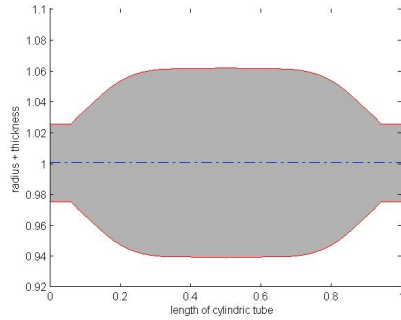


Figure 6: Configuration of the cylinder tube by Problem I

The following table shows how the error develops depending on the step size. For the unknown exact solution \bar{u}_I , we take the solution \bar{u}_{Ih} on a very fine grid with $h = 6.25 \cdot 10^{-3}$.

step-size h	$\ \bar{u}_I - \bar{u}_{Ih}\ _\infty$	$\ \bar{u}_I - \bar{u}_{Ih}\ _2$
$5.00 \cdot 10^{-2}$	$3.969554 \cdot 10^{-3}$	$1.933653 \cdot 10^{-3}$
$2.50 \cdot 10^{-2}$	$3.970259 \cdot 10^{-3}$	$1.948629 \cdot 10^{-3}$
$1.25 \cdot 10^{-2}$	$1.471205 \cdot 10^{-3}$	$1.022756 \cdot 10^{-3}$

The next table displays the discretization error of (12) in different norms.

step-size h	$\ \bar{u}_I - \bar{z}_{Ih}\ _\infty$	$\ \bar{u}_I - \bar{z}_{Ih}\ _2$
$5.00 \cdot 10^{-2}$	$1.000000 \cdot 10^{-1}$	$6.629668 \cdot 10^{-3}$
$2.50 \cdot 10^{-2}$	$1.000000 \cdot 10^{-1}$	$6.501185 \cdot 10^{-3}$
$1.25 \cdot 10^{-2}$	$2.033245 \cdot 10^{-3}$	$1.308890 \cdot 10^{-4}$

In the same way, we sketch the results for (P_{II}) and (P_{III}) .

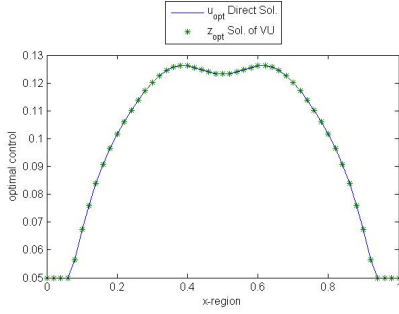


Figure 7: Optimal thickness \bar{u}_{IIh}

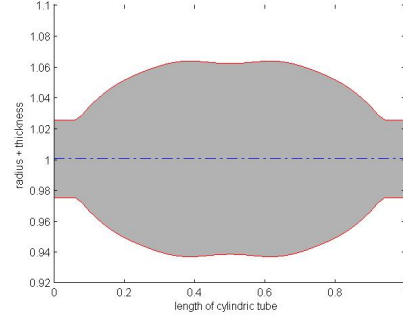


Figure 8: Configuration of the cylinder tube by Problem II

step-size h	$\ \bar{u}_{II} - \bar{u}_{IIh}\ _\infty$	$\ \bar{u}_{II} - \bar{u}_{IIh}\ _2$
$5.00 \cdot 10^{-2}$	$6.306746 \cdot 10^{-3}$	$2.278883 \cdot 10^{-3}$
$2.50 \cdot 10^{-2}$	$4.010179 \cdot 10^{-3}$	$1.194692 \cdot 10^{-3}$
$1.25 \cdot 10^{-2}$	$1.571840 \cdot 10^{-3}$	$3.023343 \cdot 10^{-4}$

step-size h	$\ \bar{u}_{II} - \bar{z}_{IIh}\ _\infty$	$\ \bar{u}_{II} - \bar{z}_{IIh}\ _2$
$5.00 \cdot 10^{-2}$	$1.036696 \cdot 10^{-3}$	$8.608683 \cdot 10^{-5}$
$2.50 \cdot 10^{-2}$	$1.033434 \cdot 10^{-3}$	$8.276054 \cdot 10^{-5}$
$1.25 \cdot 10^{-2}$	$1.032171 \cdot 10^{-3}$	$8.190915 \cdot 10^{-5}$

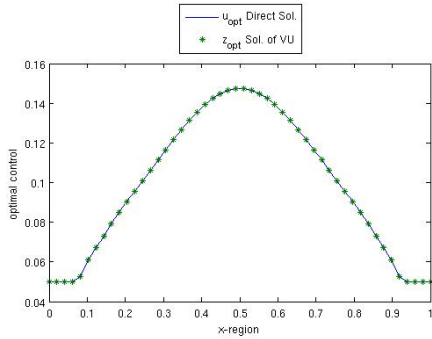
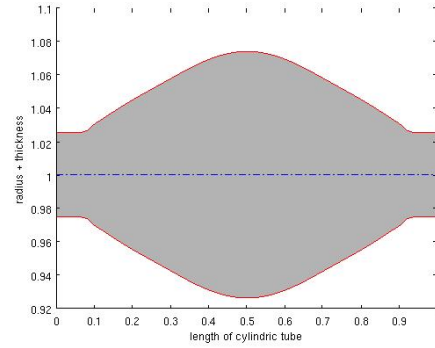
Figure 9: Optimal thickness \bar{u}_{IIIh} 

Figure 10: Configuration of the cylinder tube by Problem III

step-size h	$\ \bar{u}_{III} - \bar{u}_{IIIh}\ _\infty$	$\ \bar{u}_{III} - \bar{u}_{IIIh}\ _2$
$5.00 \cdot 10^{-2}$	$2.980146 \cdot 10^{-3}$	$7.591920 \cdot 10^{-4}$
$2.50 \cdot 10^{-2}$	$1.142223 \cdot 10^{-3}$	$3.242174 \cdot 10^{-4}$
$1.25 \cdot 10^{-2}$	$5.579242 \cdot 10^{-4}$	$2.375532 \cdot 10^{-4}$

step-size h	$\ \bar{u}_{III} - \bar{z}_{IIIh}\ _\infty$	$\ \bar{u}_{III} - \bar{z}_{IIIh}\ _2$
$5.00 \cdot 10^{-2}$	$1.057317 \cdot 10^{-3}$	$8.416476 \cdot 10^{-5}$
$2.50 \cdot 10^{-2}$	$1.056553 \cdot 10^{-3}$	$8.384105 \cdot 10^{-5}$
$1.25 \cdot 10^{-2}$	$1.056706 \cdot 10^{-3}$	$8.384590 \cdot 10^{-5}$

The solution of problem (P_{IV}) is graphically identical to that of (P_{III}), cf. Fig. 9 and 10.

Example 2. Now, the force is given by $f_z = \sin(x) \exp(t)$.

In this example we use a time-dependent and un-symmetric force. We again show the optimal control \bar{u}_{ih} and the cut trough the cylindrical shell.

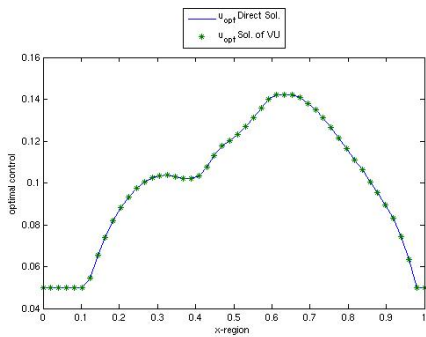
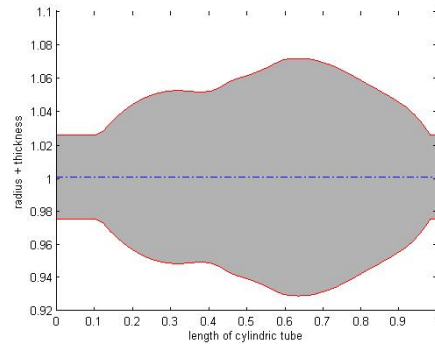
Figure 11: Optimal thickness \bar{u}_{Ih} 

Figure 12: Configuration of the cylinder tube

step-size h	$\ \bar{u}_I - \bar{u}_{Ih}\ _\infty$	$\ \bar{u}_I - \bar{u}_{Ih}\ _2$
$5.00 \cdot 10^{-2}$	$5.406534 \cdot 10^{-2}$	$8.614244 \cdot 10^{-3}$
$2.50 \cdot 10^{-2}$	$4.433849 \cdot 10^{-2}$	$1.030356 \cdot 10^{-2}$
$1.25 \cdot 10^{-2}$	$4.275253 \cdot 10^{-2}$	$3.250238 \cdot 10^{-3}$

step-size h	$\ \bar{u}_I - \bar{z}_{Ih}\ _\infty$	$\ \bar{u}_I - \bar{z}_{Ih}\ _2$
$5.00 \cdot 10^{-2}$	$8.968443 \cdot 10^{-2}$	$4.106036 \cdot 10^{-2}$
$2.50 \cdot 10^{-2}$	$9.322465 \cdot 10^{-2}$	$4.896630 \cdot 10^{-2}$
$1.25 \cdot 10^{-2}$	$4.275253 \cdot 10^{-2}$	$2.941370 \cdot 10^{-3}$

Again, we also display the results for (P_{II}) and (P_{III}) .

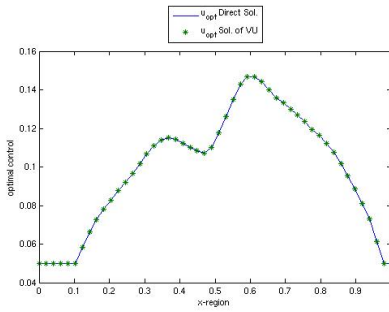


Figure 13: Optimal thickness \bar{u}_{IIIh}

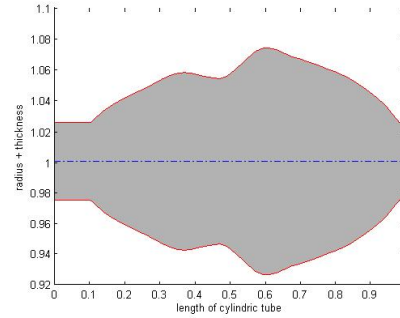


Figure 14: Configuration of the cylinder tube

We can see that the term with the mixed derivative in the original constraint has a significant influence on the optimal solutions.

step-size h	$\ \bar{u}_{II} - \bar{u}_{IIh}\ _\infty$	$\ \bar{u}_{II} - \bar{u}_{IIh}\ _2$
$5.00 \cdot 10^{-2}$	$3.525451 \cdot 10^{-2}$	$7.830259 \cdot 10^{-3}$
$2.50 \cdot 10^{-2}$	$2.291262 \cdot 10^{-2}$	$5.738711 \cdot 10^{-3}$
$1.25 \cdot 10^{-2}$	$8.049868 \cdot 10^{-3}$	$1.705603 \cdot 10^{-3}$

step-size h	$\ \bar{u}_{II} - \bar{z}_{IIh}\ _\infty$	$\ \bar{u}_{II} - \bar{z}_{IIh}\ _2$
$5.00 \cdot 10^{-2}$	$7.671809 \cdot 10^{-2}$	$3.815766 \cdot 10^{-2}$
$2.50 \cdot 10^{-2}$	$2.384418 \cdot 10^{-4}$	$6.891144 \cdot 10^{-5}$
$1.25 \cdot 10^{-2}$	$8.267400 \cdot 10^{-4}$	$7.911593 \cdot 10^{-5}$

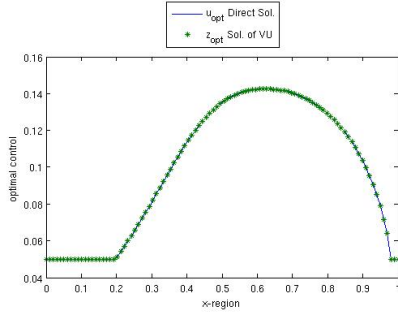
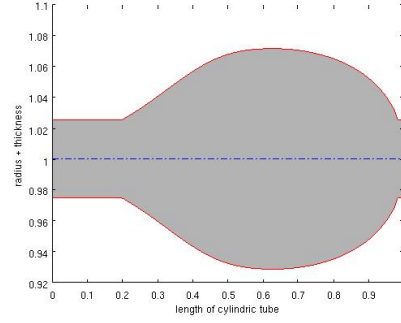
Figure 15: Optimal thickness \bar{u}_{IIIh} 

Figure 16: Configuration of the cylinder tube

step-size h	$\ \bar{u}_{III} - \bar{u}_{IIIh}\ _{\infty}$	$\ \bar{u}_{III} - \bar{u}_{IIIh}\ _2$
$5.00 \cdot 10^{-2}$	$9.322822 \cdot 10^{-3}$	$1.403460 \cdot 10^{-3}$
$2.50 \cdot 10^{-2}$	$5.215082 \cdot 10^{-3}$	$7.257135 \cdot 10^{-4}$
$1.25 \cdot 10^{-2}$	$2.969511 \cdot 10^{-3}$	$3.103673 \cdot 10^{-4}$

step-size h	$\ \bar{u}_{III} - \bar{z}_{IIIh}\ _{\infty}$	$\ \bar{u}_{III} - \bar{z}_{IIIh}\ _2$
$5.00 \cdot 10^{-2}$	$7.518352 \cdot 10^{-2}$	$1.312048 \cdot 10^{-2}$
$2.50 \cdot 10^{-2}$	$9.672485 \cdot 10^{-2}$	$1.250337 \cdot 10^{-2}$
$1.25 \cdot 10^{-2}$	$3.755295 \cdot 10^{-4}$	$5.879215 \cdot 10^{-5}$

Analogously to Example 1, the solution of problem (P_{IV}) is graphically identical to that of (P_{III}) , cf. Fig. 15 and 16.

6 Concluding Remarks

We discussed problems of optimal shape design in linear elasticity theory. The optimal thickness of a cylindrical tube is determined that minimizes the displacement of the tube under the influence of given external time-dependent force. Necessary optimality conditions for the optimal solution are formulated and proved. In contrast to previous work on this subject, we selected a direct method for the optimization for a finite element discretized model in combination with the Rothe method. We also use the finite element method to generate gradients with solution of adjoint equation and to test necessary optimality conditions. We considered only small deformations. The case of large deformations that might lead to effects of plasticity is not considered here.

References

1. P. Nestler: *Optimal Thickness of a cylindrical shell - An optimal control problem in Linear Elasticity Theory*, submitted, 2012.

2. R. T. Haftka, Z. Gürdal: *Elements of Structural Optimization*, Springer-Verlag, 11/1991.
3. Z. Mróz: *Variational methods in sensitivity analysis and optimal design*, Europ. Journ. Mech., 13, 115-147, 1994.
4. J. Sokolowski, J.-P. Zolesio: *Introduction to Shape Optimization – Shape Sensitivity Analysis*, Springer Series in Computational Mathematics 16, 1992.
5. J. Haslinger, R. A. E. Mäkinen: *Introduction to Shape Optimization: Theory, Approximation and Computation*, SIAM Philadelphia, 2003.
6. M. C. Delfour, J.-P. Zolesio: *Shapes and Geometries: Analysis, Differential Calculus and Optimization*, SIAM Philadelphia, 2001.
7. G. Rozvany: *Structural Design via Optimality Criteria*, Springer Series: Mechanics of Elastic and Inelastic Solids, Vol. 8, 1989.
8. D. Braess: *Finite Elements: Theory, Fast Solvers and Applications in Solid Mechanics*, Cambridge University Press, 2007.
9. D. Chapelle, K. J. Bathe: *The Finite Element Analysis of Shells – Fundamentals*, Springer Verlag, Berlin, Heidelberg 2003.
10. Ph. Ciarlet: *Introduction to Linear Shell Theory*, Elsevier, 1998.
11. P. Nestler: *Optimales Design einer Zylinderschale - eine Problemstellung der optimalen Steuerung in der Linearen Elastizitätstheorie*, Südwestdeutscher Verlag für Hochschulschriften, 2010.
12. J. Wloka: *Partial Differential Equations*, Cambridge University Press, 1987.
13. J. L. Lions: *Optimal Control of Systems Governed by Partial Differential Equations*, Springer-Verlag, Berlin, 1971.
14. F. Tröltzsch: *Optimal Control of Partial Differential Equations: Theory, Methods and Applications*, AMS, 2010.
15. Ph. Ciarlet: *The Finite Element Method for Elliptic Problems*, North-Holland, Amsterdam, 2000.
16. J. Sokolowski, J.-P. Zolesio: *Introduction to Shape Optimization – Shape Sensitivity Analysis*, Springer Series in Computational Mathematics 16, 1992.
17. J. Haslinger, R. A. E. Mäkinen: *Introduction to Shape Optimization: Theory, Approximation and Computation*, SIAM Philadelphia, 2003.
18. M. C. Delfour, J.-P. Zolesio: *Shapes and Geometries: Analysis, Differential Calculus and Optimization*, SIAM Philadelphia, 2001.

19. St. P. Timoshenko: *Vibration Problems in Engineering*, D. Van Nostrand Company, 1st Ed. 1928.
20. J. Sprekels, D. Tiba: *Optimization problems for thin elastic structures*, in "Optimal Control of Coupled System of PDE", ISBNM Birkhäuser, 2009, 255-273.
21. P. Nestler: *Calculation of deformation of a cylindrical shell*, Greifswalder Preprintreihe Mathematik, 4/2008.
22. P. Nestler, W. H. Schmidt: *Optimal Design of Cylindrical Shells*, *Discussiones Mathematicae, Differential Inclusions, Control and Optimization* 30(2010), 253-267.